The new real-time measurement capabilities of the profiling TARA radar

Christine Unal

Christine Unal, Yann Dufournet, Tobias Otto and Herman Russchenberg
Geoscience and Remote Sensing, TU-Delft Climate Institute, Stevinweg 1, 2628 CN Delft, Netherlands, c.m.h.unal@tudelft.nl

1. Introduction

In the past 10 years, the S-band FM-CW TARA (Transportable Atmospheric RAdar), placed at the Cabauw Experimental Site for Atmospheric Research (CESAR), provided in real-time vertical profiles of the Doppler moments. Classical spectral processing was carried out. The polarimetric and multi-beam measurement capabilities of the radar were not exploited in real-time. It was only possible to acquire raw data for case studies. Based on them, new algorithms were developed using spectral polarimetry and the multi-beam capability of TARA. They have been tested during the COPS (2007) and EUCAARI-IMPACT campaigns (2008).

To measure in real-time the Doppler moments of three beams, the differential reflectivity, the linear depolarization ratio, the horizontal wind and the vertical mean Doppler velocity, it became necessary to upgrade TARA. This resulted in a new design of the radar control unit and a new processing based on spectral polarimetry. This major upgrade took place in 2011. TARA can now deliver multi-parameters profiles with high spatial and time resolution and raw data in real-time. They are stored with the NetCDF format. Furthermore, detailed quick-looks of all the observables are available in real-time at http://ftp.tudelft.nl/TUDelft/irctr-rse/tara/index.html.

For the design of the radar control unit and processing, a flexible solution that can process the data in a high level programming language, was chosen. This was done to be able to easily implement future developments in radar signal processing and algorithms.

2. System description

The radar system is based on the FM-CW principle (Frequency Modulated Continuous Wave). It uses a digitized linear frequency sweep of maximally 50 MHz (3 m range resolution). The range resolution, from 3 to 30 m, and related maximum range can be selected by the user. The standard measurement mode uses the 30 m range resolution and 15 km maximum range. The standard mode consists of the continuous repetition of a cycle of 5 different measurements (VV, HV, HH, OB1, OB2) using the smallest sweep time of 0.5 ms, which means that polarimetric (VV, HV, HH) and multi-beam (VV, OB1, OB2) sequence is obtained within 2.5 ms (T_m). Using dealiasing techniques, the maximum unambiguous Doppler velocity is increased from 9 m s^{-1} ($v_{D,max}$) to 45 m s^{-1} for the polarimetric main beam and from 9 m s^{-1} to 27 m s^{-1} for the single-polarised offset beams. The Doppler resolution is 3.6 cm s^{-1} and the time resolution of the profiles is 2.56 s.

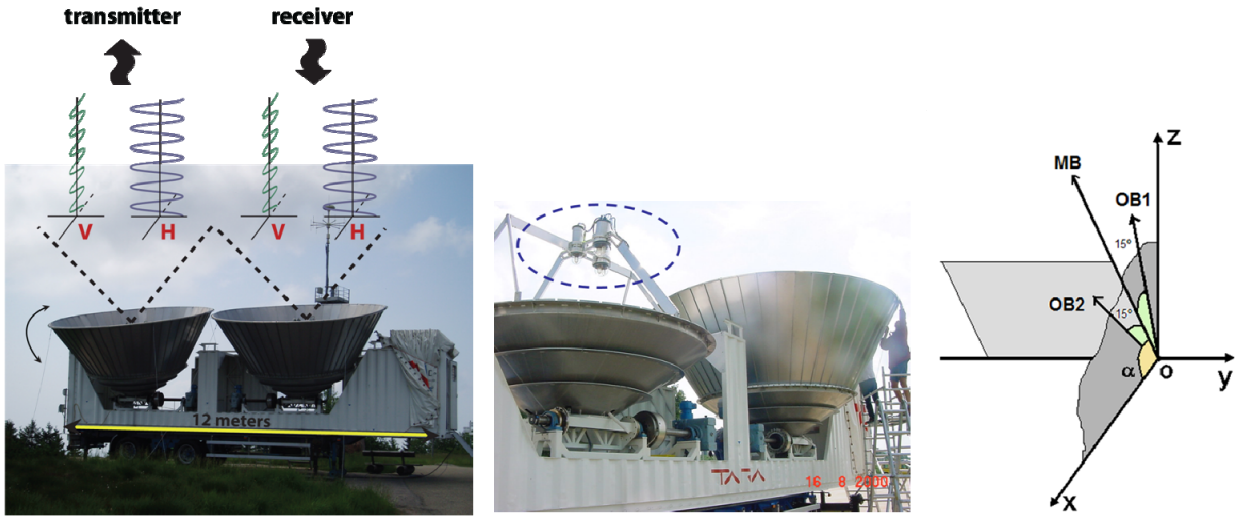

Fig. 1 Transportable Atmospheric RAdar (TARA): general view (left), antennas and the 3 feeds (middle), local coordinate system (right) where X is the azimuth direction of the main beam (MB) and Z the vertical direction.

Isolation between the transmitter and the receiver is realized by the use of two separate antennas with large shields. Each antenna has three feeds. One beam is directed along the axis of symmetry of the parabolic reflector. This beam is dual-polarized. Two off-axis beams at an angle of 15 deg. in two orthogonal directions are generated with small off-focus placed feed arrays. They are single-polarized. These beams are used in conjunction with the central beam (MB) to estimate the 3D wind field. The antennas have a symmetrical pattern in the E- and H-plane with a beam width of 2.1 deg and an antenna gain

of 38.8 dBi. Each antenna is controlled independently. As the central feed is dual-polarized, the full scattering matrix can be measured from three measurements (single channel receiver). The cross polar isolation of the antennas is -29 dB for distributed targets. The elevation α can vary from 0 to 90 deg. Fig. 1 depicts TARA with its antennas.

The maximum transmit power of TARA is 100 W. The power out of the antenna is 36 W due to losses in cables and the beam forming network. Because of receiver saturation, the transmit power can be attenuated by 10 dB steps in case of heavy precipitation.

3. Design of the radar control and processing

The main requirements of the new design of the radar control unit and processing, are flexibility of the system and the ability to directly use developed Matlab codes. Parts of the new design are a PXI, Labview software, a DDS (Direct Digital Synthesizer) and Matlab codes. The signal is defined by user input (range resolution, measurement cycle, …) and generated by the DDS. The main tasks of the PXI are timing and synchronization in the radar control unit, and the analog to digital conversion of the received signal. The Labview software is employed for the radar control unit and the graphical interface. It uses Matlab codes for the data processing and the data storage in NetCDF files (processed data, noise data, raw data).

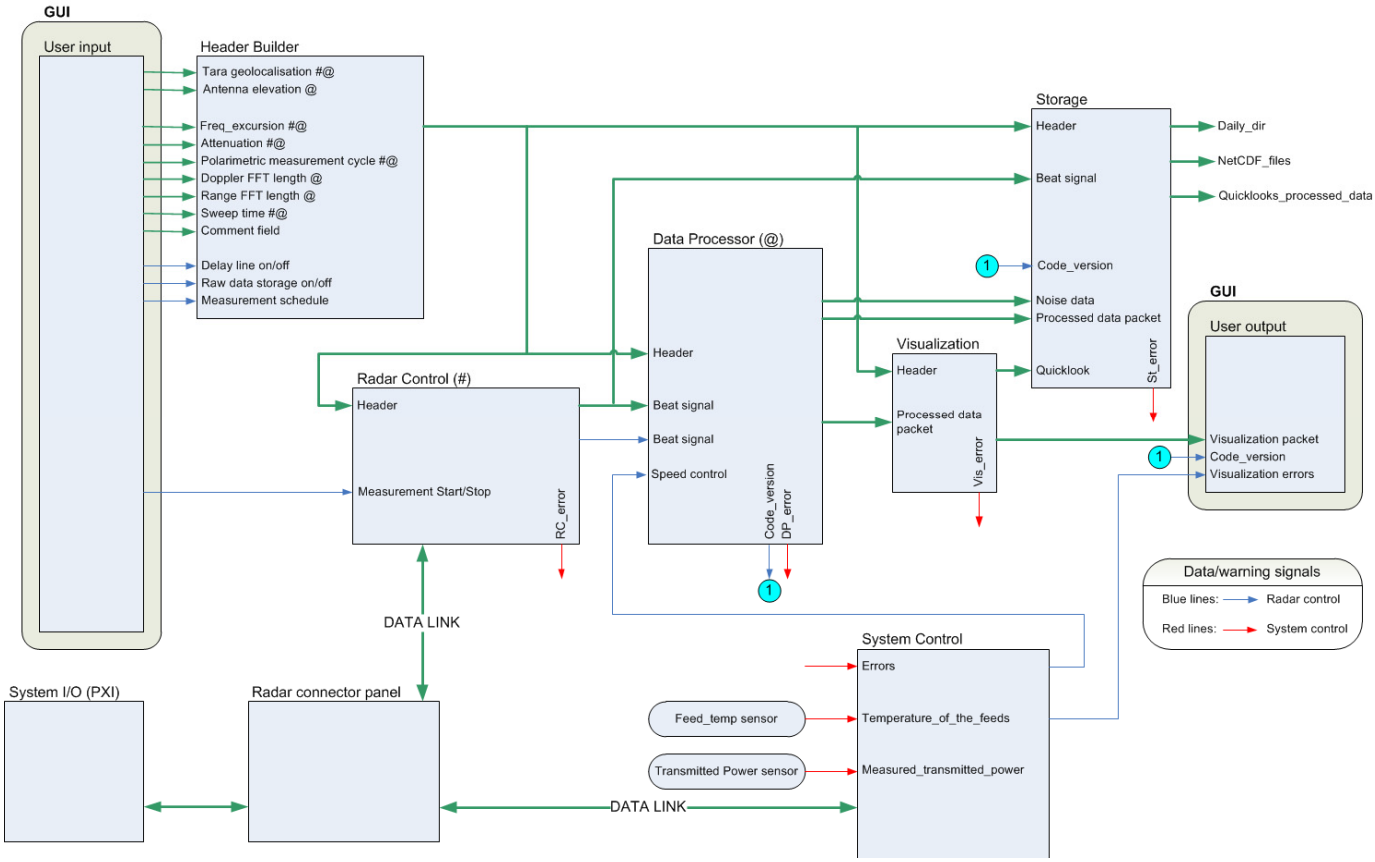

Fig. 2 TARA general block diagram of the radar control unit and processing

The diagram of the radar interface, represented in Fig. 2, shows the signals that each block within the interface send out to other blocks and which signal it needs to receive (van Gemert et al. 2011, den Engelsen and Stienstra 2011). It consists of the following seven blocks:

1) GUI (Fig. 3)

2) Header builder: the header builder takes all the measurement settings that are set in the GUI and bundles them together so they can be easily transmitted. All variables present in the header builder block are fixed and set only once before the measurement. The radar control needs the measurement settings to tell the PXI and consequentially the radar what type of measurement must be done. The data processor needs them in order to correctly process the beat signal, the visualization needs to know what exactly to display and the storage block needs to store the measurement settings together with the data that is to be saved.

3) Radar control: the radar control block is designed to control and receive signals from the radar and start each of the other blocks when they are needed. Also, through the connection with the radar connector panel, it is able to send signals to the PXI. By doing this, the radar control block can instruct the PXI to create the type of beat signal that is required for the noise measurement or the 3 (polarimetric), 5 (polarimetric + wind) or customized cycle of measurement.

4) Data processor: the task of the data processor is to process the beat signal in order to extract atmospheric echoes that are received by the radar, so they can be stored and displayed. The processing is only performed in case of 3 or 5 measurements cycle. If the beat signal is of a custom measurement configuration, it will not be processed and only raw data will be stored. At the start of every measurement, a beat signal containing only noise is sent to the data processor. This

noise signal is processed and 2 sets of variables are delivered of which the first one is used to filter out the noise in the upcoming measurements and the second one supplies a range dependent calibration constant. These 2 variables are sent to the storage block as noise data. After the noise has been processed, the data processor receives a beat signal for either a cycle of 3 or 5 measurements and then needs to process them with the appropriate Matlab code. The processed data that is created are then sent to storage and to visualization to display them. The sub-blocks of the data processor also send a string with the Matlab code version along with the data.

5) Visualization: the visualization block has to create packets of data which the GUI can interpret and display in graphs. It also needs to create the quicklooks that need to be saved. Up to 15 processed radar observables are sent out as visualization packet to the GUI. Each of the processed observables is height and time dependent (represented as 2D matrices).

6) Storage: 4 types of data packages can be stored:

- a noise package which consists of the header, processed and raw noise data from a noise measurement of 1 min and 1 min of raw data measured with power transmission.
- a transmission package, which consists of the header and the processed data
- a raw data package which consists of the header and raw data.
- a quicklook package.

To be able to deal with different packages at the same time, several buffers are considered to be used in parallel after the merging of the required data has been done. When the buffers are full, the data are written in NetCDF format. Finally the data are stored into several package dedicated folders present on the hard disk. These folders are also placed within daily classified directories. This folder classification tree is handled and created by the storage block itself. The storage block also has its own control block. This block is notified if the day is at an end, so that new file for a new day of measurements can be created. It also receives a signal which indicates what packages the user wants to save as well as a signal that tells the storage block that the measurement has been stopped and it needs to save the data.

7) System control: the system control block is there to receive and process errors. When one of the sub-blocks of the system runs into problems it outputs an error to the system control block. This block then outputs the error to the user through the GUI and in the worst case it sends a signal to the radar connector panel to shut down the radar.

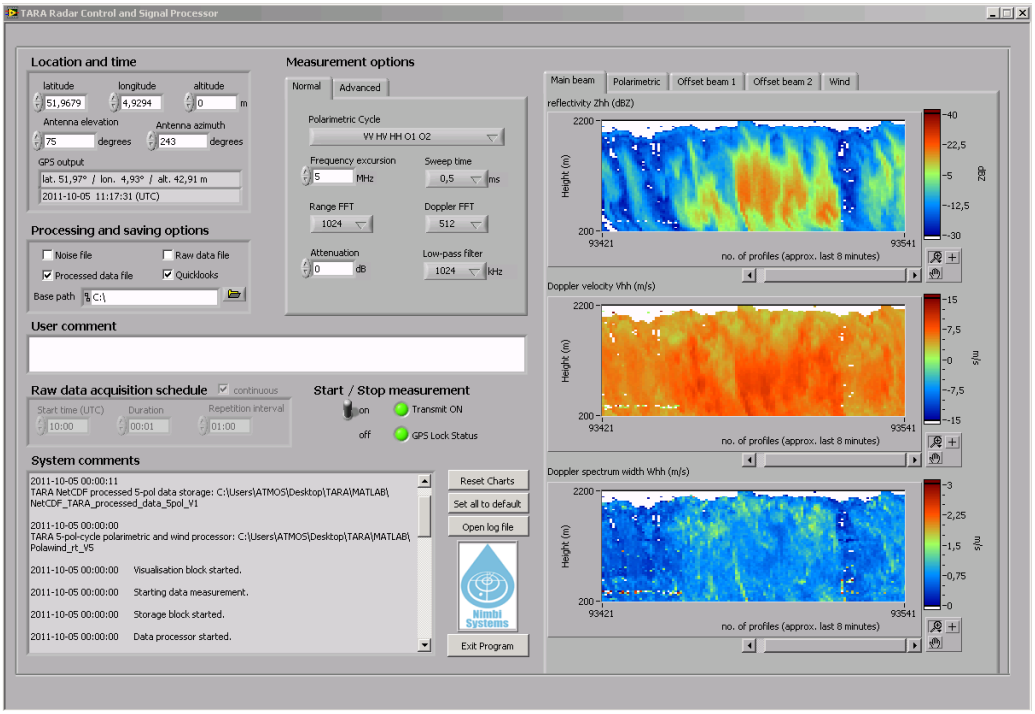

Fig. 3 GUI: example of real-time measurement acquisition. It shows convective light rain measured by the main beam.

4. Real-time data processing using spectral polarimetry

The three beams capability of TARA permits to acquire three Doppler spectra in three different directions to calculate the wind field. Because of the importance of a correct estimate of the vertical Doppler velocity, one beam (OB1) is looking at the zenith while the two other beams are respectively at α=75 deg (MB) and 69 deg (OB2) of elevation in the standard wind mode. We employ the following acquisition sequence, MB (*VV*, *HV*, *HH*), OB1 (*VV*) and OB2 (*VV*). Doppler processing (with Hamming window) is carried out on the 5 time series for each radar resolution volume. It was shown in (Dufournet 2010, ch. 4 p. 46) that the Doppler moments converge to a stable value from the Doppler FFT-length, L=256, in the case of precipitating cloud. To choose the upper boundary for the FFT-length a trade-off (512) has been made between the number of data with high signal-to-noise ratio necessary for microphysical retrievals carried out directly on the spectrograms (Spek et al. 2008, Unal 2012) and the increase of statistical fluctuations with L. Adding dual-polarization measurements for clutter

suppression adversely affects the measurable maximum unambiguous velocity. Therefore dealiasing techniques have been implemented to palliate this limitation.

4.1 Doppler dealiasing

The polarimetric dealiasing is discussed in details by (Unal and Moisseev 2004). This method allows to perform consecutive polarimetric and wind measurements with the maximum unambiguous Doppler velocity of a single measurement (sampling time $T_m/5$). The technique is based on the spectral differential phase which has a probability density function (pdf) centered in 0 for atmospheric targets in the case of S-band profiling radar and no aliasing. When the pdf shows multi-peaks (in general two), the peak phase values are related to the actual Doppler velocity interval of the atmospheric targets. Prior to the dealiasing operation, the spectral differential phase has to be compensated because of the non-simultaneity of the polarimetric measurements. The consequence of this method is to remove the atmospheric targets with a spectral cross-correlation inferior to 0.78 after averaging two consecutive spectral covariance matrices. Therefore clutter and noise are already partially removed. This technique is only valid for the polarimetric beam. However, as soon as one correct profile of mean Doppler velocity is obtained, it can be used to dealiase the Doppler spectra of the single-polarized beams.

When the beam is single-polarised, the Doppler spectrum is declared folded or not folded searching for signal at the edges of the spectrum (signal-to-noise ratio larger than 3 dB after smoothing). An unfolding procedure is then applied on the folded Doppler spectrum using the location of the maximum power of the smoothed signal. The second processing step is range continuity using cross-correlation of the Doppler spectra. The critical part is the selection of a reference Doppler spectrum. Because its mean Doppler velocity has low values in the case of a vertical profile, a cloud Doppler spectrum is searched (precipitation). From the highest height, the first Doppler spectrum not folded, with sufficient SNR (3 dB) and a related Doppler width smaller than 1.8 m s^{-1} is chosen as a reference. The value 1.8 m s^{-1} is the mean Doppler width of rain measured at high elevation in the atmospheric site Cabauw (The Netherlands), where TARA is usually located. For the cases drizzle, where the water cloud cannot be measured at S-band due to the small sizes of water droplets (μm), and clear air echoes, the highest drizzle and the top of the boundary layer Doppler spectrum is quoted as reference by the algorithm.

Prior to the selection of a reference Doppler spectrum, the individual Doppler spectra may be shifted in the Doppler velocity interval by ± 2 $v_{D,max}$ in the case of slant profiling of precipitation when the dealiased mean Doppler velocity of the polarimetric beam exceeds a threshold (strong horizontal wind). In that case, a cloud Doppler spectrum, previously folded, can be a reference for the range continuity of the spectrogram.

4.2 Spectral clutter and noise reduction

For the polarimetric beam, three complex Doppler spectra $S_{VV}(r,v)$, $S_{HV}(r,v)$ and $S_{HH}(r,v)$ are obtained each 2.56 s, r being the range, v the Doppler velocity, and VV, HV and HH the polarization settings. From them spectral polarimetric parameters can be estimated like the spectral linear depolarization ratios:

$$sL_{dr}^{HH}(r,v) = 10\log\left(\frac{\left\langle S_{HV}(r,v)S_{HV}^{*}(r,v)\right\rangle}{\left\langle S_{HH}(r,v)S_{HH}^{*}(r,v)\right\rangle}\right) = 10\log\left(\frac{\left\langle sZ_{HV}(r,v)\right\rangle}{\left\langle sZ_{HH}(r,v)\right\rangle}\right) \qquad (1)$$

$$sL_{dr}^{VV}(r,v) = 10\log\left(\frac{\left\langle S_{HV}(r,v)S_{HV}^{*}(r,v)\right\rangle}{\left\langle S_{VV}(r,v)S_{VV}^{*}(r,v)\right\rangle}\right) = 10\log\left(\frac{\left\langle sZ_{HV}(r,v)\right\rangle}{\left\langle sZ_{VV}(r,v)\right\rangle}\right) \qquad (2)$$

where < > indicates time averaging of the power Doppler spectra and sZ represents the spectral reflectivity. Both parameters (1) and (2) are employed to suppress clutter and noise in the Doppler spectra of atmospheric targets (Unal 2009). For this purpose, a clipping threshold of –5 dB is selected. All the Doppler velocity bins of the complex Doppler spectra, which correspond to $sL_{dr}^{HH}(r,v) > -5$ dB or $sL_{dr}^{VV}(r,v) > -5$ dB, are discarded. The important advantage of this double sL_{dr} filter consists of suppressing more clutter than a single sL_{dr} filter, without further removing atmospheric target echoes. The noise signal is censored as well since the noise means,

$$\overline{sL_{dr}^{HH}(r,v)} = \overline{sL_{dr}^{VV}(r,v)} = 0 \text{ dB} \qquad (3)$$

Applying both thresholds is very effective for noise suppression after a small average of the power Doppler spectra, namely 2, because both $sL_{dr}(r,v)$ are not correlated for the noise. The result is a spectrogram of atmospheric targets nearly free of clutter and noise.

For the single-polarized beams, the noise signal is censored by only keeping the Doppler bins of which the spectral reflectivity is larger than 5 dB above the mean spectral noise floor. Further a notch filter, which removes the Doppler bin interval [–0.2, 0.2] m s^{-1}, suppresses the ground clutter. This interval is experimentally obtained for the range of elevations 45-90 deg in the site Cabauw. In the boundary layer when no precipitation occurs, range-Doppler areas quoted as clutter by the polarimetric beam, are removed in the offset beams spectrograms.

4.3 From spectrograms to wind profiles

At this stage of the processing, the spectrograms can be directly considered as inputs for microphysical retrievals (Spek et al 2008, Unal 2012) and they can be used to calculate profiles of the Doppler moments and polarimetric parameters. For the wind estimation, three mean Doppler velocity profiles are calculated from the three-beam spectrograms. They are related to

the resolution volume heights, which differ with the beam. Therefore the height series of the polarimetric beam is chosen as reference and the profiles of mean Doppler velocity of the single-polarized beams are linearly height-interpolated. Next, geometrical transformations are applied to compute the wind components (V, U, W). The end products are the profiles of the mean vertical Doppler velocity W (also in the case of slant profiling), the horizontal wind speed v_H and direction D.

The wind estimation is carried out when data are available for the three beams. Therefore if some mean Doppler velocities are biased by clutter in the case of the single-polarized beams, they may not be employed to estimate the horizontal wind and the final vertical velocity because there is no data for the polarimetric beam. This is an indirect spectral polarimetric filtering. Finally a mask based on the Doppler width is applied on the profiles. Radar observables corresponding to a Doppler width inferior to the Doppler resolution and superior to 3 m s^{-1} are discarded.

The profiles start just below 200 m to censor the radar near-field and partial overlapping of the two antennas of TARA. For the latter, a range correction on the reflectivity is implemented.

5. Real-time measurement example

The GUI real-time visualization plots are captured to be seen via the internet link http://ftp.tudelft.nl/TUDelft/irctr-rse/tara/index.html every minute and stored. The reflectivity of the horizontal scanning X-band radar IDRA (Figueras i Ventura, 2009), which is located on the same site can also be seen, as well as the image of the webcam placed in the looking direction of the main beam of TARA. TARA profiles will be placed soon in the CESAR database (http://www.cesar-observatory.nl). Like IDRA data, they will be freely available.

When the measurements are foreseen to be particularly interesting, raw data are also acquired to investigate the Doppler spectra. That is the case of the 3rd January of 2012, when a heavy cold front passing over the site could be observed and monitored (see synoptic situation of Fig. 4a).

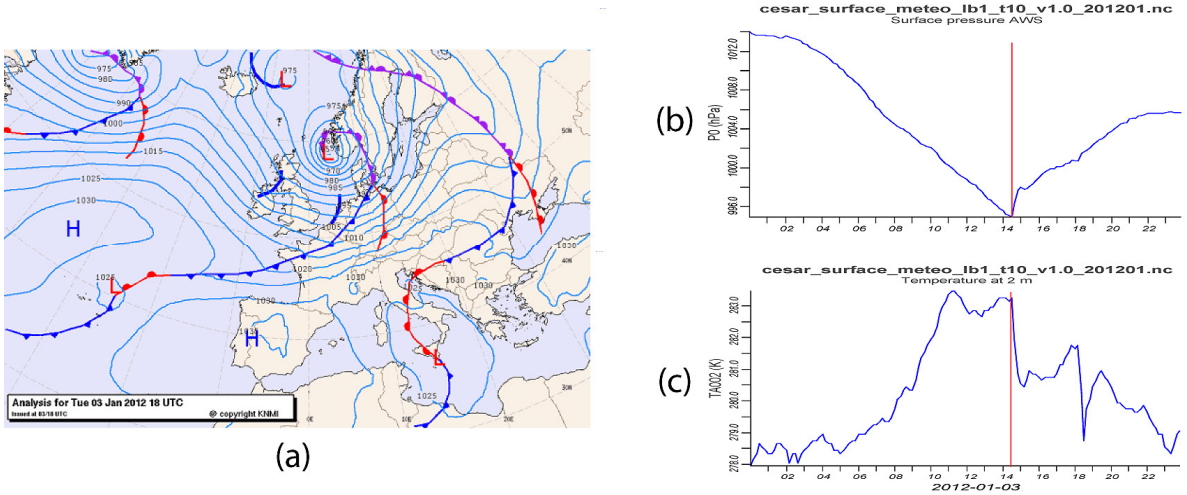

Fig. 4 Weather situation on January 3rd, 2012. (a) Synoptic situation of the frontal activity as analyzed by KNMI. (b) Evolution of surface pressure at the CESAR observation site from 00:00 UTC to 23:50 UTC. (c) Evolution of temperature at 2m at the CESAR observation site from 00:00 UTC to 23:50 UTC (the red line depict the overpass of the cold front)

Figure 5 displays the real time measurement gathered during this event by the two TU DELFT IDRA and TARA radars. On the left side of the figure, the mesoscale evolution of the precipitation pattern is well captured around the site by the IDRA PPIs updated every minute. Of particular interest is the detection and evolution of a thin line of strong reflectivity at the frontal edge where heavy precipitation is occurring. This convergence line arrived at the site of Cabauw from the North-West direction. The temporal evolution of the frontal system over the site is, on the other hand, well observed on the TARA measurements profiles on the right side of Fig. 5.

Before the frontal edge passed over the site, a stratiform rain regime could be observed with the presence of a melting layer well detected by TARA (strong reflectivity line at about 1.8 km height associated with larger linear depolarization ratio of -15 to -20 dB compared to rain). From 14.71 to 14.74 UTC, the melting layer seemed to be lifted up to 2.2 km as observed in the LDR profiles. This is probably due to the convergence of the two air masses, the warmest one (less dense), south east of the frontal edge on the IDRA PPI and left of the TARA profiles, being forced to be lifted up by the other (coldest and densest) air mass, as typically observed during a cold front overpass. Both air masses are also well observed on Fig. 4c with a temperature drop of about 2°K detected when the front is passing over the site, referring to a change in the air mass properties. It is worth noticing that although an updraft is probably occurring, TARA vertical Doppler velocities within this time frame showed large negative values, typical of downward motion of cloud system hydrometeors. Strong reflectivities observed in this downward motion region suggest that large hydrometeors were present reaching a large fall speed velocity and counteracting the uplift velocity of the air mass. The warm air mass lifting was therefore only inferred by the height change of the melting of the ice particles observed in the LDR profile, due to warmer temperature in higher altitudes.

At about 14.74 UTC, the frontal edge passed over the site. The sharp air mass convergence produced a strong updraft beneficial for the large production of cloud hydrometeors (well correlated with the pressure minimum observed on Fig. 4b). Such convergence line was combined with heavy turbulence (as determined by the large Doppler spectrum width values observed at that time), most probably favoring heavy aggregation processes resulting to the production of large

hydrometeors and heavy rainfall. This hypothesis was validated with the strong reflectivity values observed in both TARA and IDRA measurement suggesting the presence of large hydrometeors.

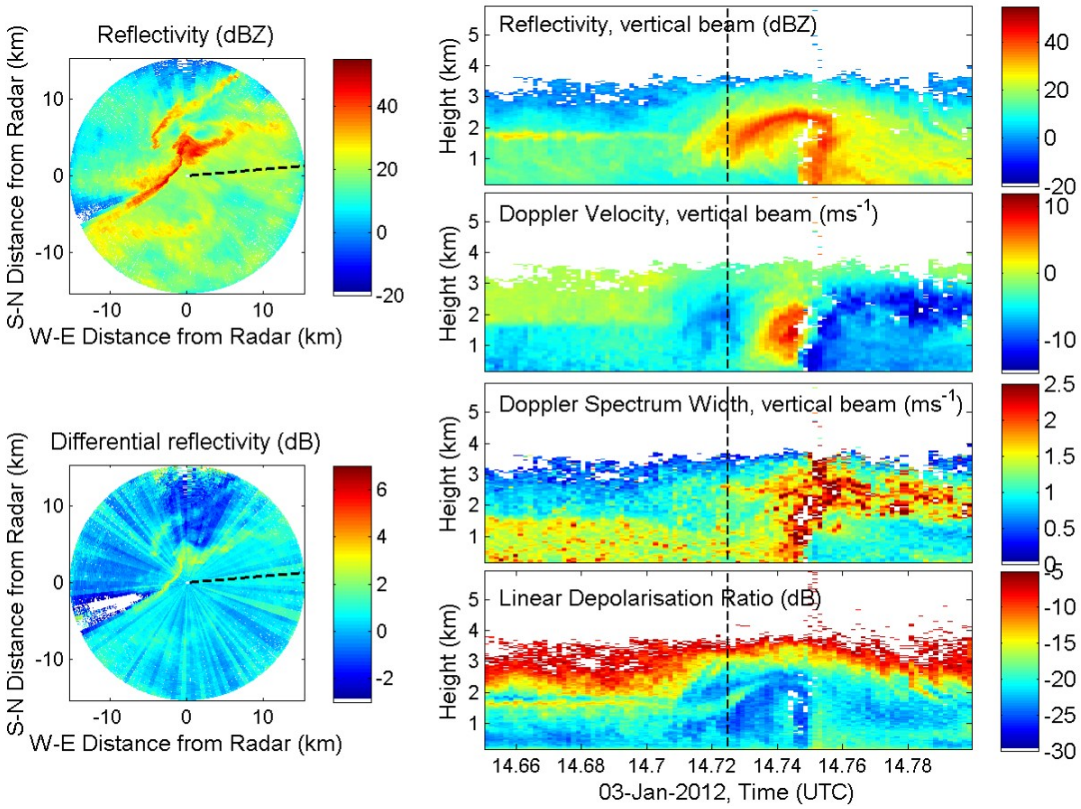

Fig. 5 Measurement example of high time and range resolution of TARA profiling vertically and IDRA profiling horizontally. TARA is located 339 m away from IDRA. The time scale of TARA is about 8 min. The linear depolarization ratio is measured by the main beam at 75 deg elevation. IDRA PPI's are here not yet corrected for attenuation.

From 14.75 UTC, the frontal line (between the two air masses) seems to be well characterized by the turbulence contrast observed in the Doppler spectrum width values. Of particular interest is the heavy downward Doppler velocity associated with the frontal line. It is most probably the signature of a so-called cold pool formation. In that region, heavy precipitation formed at the frontal edge might be mixed with the colder (and dryer) air mass, producing strong evaporative cooling. The cooled air mass got heavier, enhancing the fall velocity of the hydrometeors. Such event occurred in less than 8 min and therefore high temporal resolution provided by TARA was required.

Acknowledgments

The authors would like to thank the five students team: Enzo den Engelsen, Jeroen van Gemert, Martijn Janssen, Satoshi Malotaux and Esther Stienstra for the design and implementation of the new TARA real-time interface. We want also to thank the radar technical team, Fred van der Zwan and Paul Hakkaart for their advices and assistance.

References

Dufournet Y., 2010: *Ice crystal properties retrieval using spectral polarimetric measurements within ice/mixed-phase clouds*, PhD thesis, Delft University of Technology, 138 p.

den Engelsen E., Stienstra E., 2011: *Designing for TARA, data processing, visualization and storage*. Bachelor thesis, Delft University of Technology.

Figueras i Ventura J., 2009: *Design of a high resolution X-band Doppler polarimetric weather radar*, PhD thesis, Delft University of Technology, 162 p.

Van Gemert J., Janssen M., Malotaux S., 2011: *Designing for TARA, the radar control unit*. Bachelor thesis, Delft University of Technology.

Spek A., Unal C., Moisseev D., Russchenberg H., Chandrasekar V., Dufournet Y., 2008: A new technique to categorize and retrieve the microphysical properties of ice particles above the melting layer using radar dual polarization spectral analysis. *J. Atmos. Oceanic Technol.,* **25**, 482-497

Unal C., 2009: Spectral polarimetric radar clutter suppression to enhance atmospheric echoes . *J. Atmos. Oceanic Technol.*, **26**, 1781-1797.

Unal C. M. H., Moisseev D. N., 2004: Combined Doppler and polarimetric radar measurements: correction for spectrum aliasing and non simultaneous polarimetric measurements. *J. Atmos. Oceanic Technol.*, **21**, 443-456.

Unal C., 2012: Multi-beam raindrop size distribution retrievals on the Doppler spectra. Preprints, *Seventh European Conf. on Radar in Meteorology and Hydrology (ERAD)*, Toulouse, France.